

# No evidence of chemical anomalies in the bimodal turnoff cluster NGC 1806 in the LMC <sup>1</sup>

A. Mucciarelli<sup>1</sup>, E. Dalessandro<sup>1</sup>, F. R. Ferraro<sup>1</sup>, L. Origlia<sup>2</sup>, B. Lanzoni<sup>1</sup>

<sup>1</sup>*Dipartimento di Fisica & Astronomia, Università degli Studi di Bologna, Viale Berti Pichat, 6/2 - 40127 Bologna, ITALY*

<sup>2</sup>*INAF - Osservatorio Astronomico di Bologna, via Ranzani, 1 - 40127, Bologna, ITALY*

## ABSTRACT

We have studied the chemical composition of NGC 1806, a massive, intermediate-age globular cluster that shows a double main sequence turnoff. We analyzed a sample of high-resolution spectra (secured with FLAMES at the Very Large Telescope) for 8 giant stars, members of the cluster, finding an average iron content of  $[\text{Fe}/\text{H}] = -0.60 \pm 0.01$  dex and no evidence of intrinsic star-to-star variations in the abundances of light elements (Na, O, Mg, Al). Also, the  $(m_{F814W}; m_{F336W} - m_{F814W})$  color-magnitude diagram obtained by combining optical and near-UV Hubble Space Telescope photometry exhibits a narrow red giant branch, thus ruling out intrinsic variations of C and N abundances in the cluster. These findings demonstrate that NGC 1806 does not harbor chemically distinct sub-populations, at variance with what was found in old globular clusters. In turn, this indicates that the double main sequence turnoff phenomenon cannot be explained in the context of the self-enrichment processes usually invoked to explain the chemical anomalies observed in old globulars. Other solutions (i.e., stellar rotation, merging between clusters or collisions with giant molecular clouds) should be envisaged to explain this class of globulars.

*Subject headings:* stars: abundances — globular clusters: individual (NGC 1806) — Magellanic Clouds — techniques: spectroscopic — techniques: photometric

## 1. Introduction

Several intermediate-age (1-3 Gyr) globular clusters (GCs) in the Large and Small Magellanic Clouds (LMC and SMC) exhibit an extended main sequence turnoff (MSTO) in their optical color-magnitude diagrams (CMDs). The observed spread can appear either as a broad region or as a

---

<sup>1</sup>Based on observations collected at the ESO-VLT under the program 084.D-0933 and collected with the NASA/ESA HST, obtained at the Space Telescope Science Institute, which is operated by AURA, Inc., under NASA contract NAS5-26555.

clear bifurcation, while the MS and red giant branch (RGB) appear well defined and narrow in the optical CMDs. By using Hubble Space Telescope (HST) photometry Mackey & Broby Nielsen (2007) first detected two distinct MSTOs in the massive, intermediate-age LMC GC NGC 1846 and in the last few years the list of GCs with anomalous MSTO morphologies has grown significantly (see e.g. the sample of 16 LMC GCs discussed by Milone et al. 2009). According to the observed MSTO morphology, three classes of intermediate-age Magellanic clusters can be distinguished: (1) GCs with a narrow MSTO, with the massive GC NGC 1978 as prototype (Mucciarelli et al. 2007); (2) GCs with a broad MSTO but no clear bimodality; (3) GCs with a bimodal MSTO. Out of 16 GCs studied by Milone et al. (2009), five belong to class (1) and eight to class (2). Examples of clusters with bimodal MSTO are NGC 1751, NGC 1806, NGC 1846 in the LMC (Mackey et al. 2008; Milone et al. 2009; Goudfrooij et al. 2009) and NGC 419 in the SMC (Glatt et al. 2008).

In GCs where distinct sequences are observed, population ratios and radial distributions have been studied with results that are still debated and controversial. For example, Goudfrooij et al. (2009) found that the brightest MSTO stars in NGC 1846 are more centrally concentrated than the faintest ones. Instead, in NGC 1783 the faintest MSTO stars are more centrally concentrated (Rubele et al. 2013). Finally, at least in the cases of NGC 1806, NGC 1846 and NGC 1751, the brightest MSTO appears to be more populated with respect to the faintest one (Milone et al. 2009).

Spurious effects due to differential reddening, field star contamination or photometric uncertainties have been deeply investigated and ruled out (see e.g. Mackey et al. 2008; Goudfrooij et al. 2011a) and different scenarios to explain the observed MSTO have been envisaged. In particular it has been proposed that the extended MSTOs could reflect a real age difference, thus suggesting that these clusters have undergone prolonged (continuous or bursty) star formation activity (see e.g. Goudfrooij et al. 2009; Milone et al. 2009; Keller et al. 2011). Within this framework, the ages should range between  $\sim 50$  and  $\sim 300$  Myr (Milone et al. 2009). An alternative explanation could be that an extended MSTOs are due to the presence of fast rotating MS stars, which are predicted to evolve at lower effective temperatures (thus redder colors) with respect to non-rotating MS stars. However, conflicting results about the efficiency of this effect have been found so far (see e.g. Bastian & de Mink 2009; Girardi et al. 2011). Finally, through merging and mass transfer processes, interactive binaries can also produce an extension of the MSTO toward bluer colors and brighter magnitudes (Yang et al. 2011). However, this could only partially explain the broad MSTOs (under the strong assumption that all the cluster stars are members of binary systems; Yang et al. 2011), but this scenario is unable to account for the bimodal MSTO.

In the first case, Goudfrooij et al. (2009) and Keller et al. (2011) proposed a connection between the double/broad MSTO and the self-enrichment processes invoked to explain the chemical anomalies in the light elements abundances commonly observed in old, massive GCs (see e.g. Gratton et al. 2012, and references therein). In the generally accepted scenario (see e.g. Ventura et al. 2001; D’Ercole et al. 2008; Decressin et al. 2010; Valcarce & Catelan 2011), the currently old and massive GCs underwent prolonged star formation activity in their early stage, over a period smaller than  $\sim 200$ -300 Myr. Thus, *second generation* stars formed from a gas processed

by the CNO cycle and ejected by first generation stars, like asymptotic giant branch (AGB) and/or fast-rotating massive stars<sup>2</sup>. Following this scenario, the dual/broad MSTOs would be direct evidence of prolonged star formation activity occurring in the early stages of GC formation (which is not observable in the CMDs of old GCs because the age spread is negligible with respect to the cluster age). As a consequence, Magellanic GCs with dual/broad MSTO should exhibit intrinsic star-to-star variations in the abundances of the elements involved in the complete CNO cycle (C, N, O, Na, Mg, Al).

The aim of this Letter is to test this scenario, searching for the expected chemical anomalies in the massive GC NGC 1806 ( $M=1.07\cdot10^5 M_{\odot}$ , Goudfrooij et al. 2011b), which shows a well-defined bimodal MSTO (Mackey et al. 2008).

## 2. Observations and data reduction

In order to investigate possible chemical anomalies in the abundances of light elements of NGC 1806, we analyzed high-resolution spectra to derive O, Na, Mg and Al abundances, and high-resolution photometric data to study C and N abundances.

– *The spectroscopic data set:* High resolution spectra have been obtained with the multi-object facility FLAMES (Pasquini et al. 2000) at the Very Large Telescope of the European Southern Observatory in the UVES+GIRAFFE combined mode. The targets have been selected from the near-infrared catalog of Mucciarelli et al. (2006) for the innermost region (within  $\sim 2.5'$  from the cluster center) and from the 2MASS catalog (Skrutskie et al. 2006) for the external region. The UVES fibers have been allocated in the circular corona between  $\sim 20''$  and  $\sim 60''$  from the cluster center. The GIRAFFE fibers have been allocated in the surrounding field and only a few of them close to the cluster center (note that the small angular size of the cluster, combined with the physical size of the magnetic button supporting the FLAMES fibers, prevents the allocation of more than  $\sim 12$  fibers in the central region). The UVES targets were observed with the Red Arm 580 grating ( $\sim 4800$ - $6800 \text{ \AA}$ ), while the GIRAFFE targets with the HR11 ( $\sim 5600$ - $5800 \text{ \AA}$ ) and HR13 ( $\sim 6100$ - $6400 \text{ \AA}$ ) gratings. Both the UVES and GIRAFFE spectra were reduced using the dedicated ESO pipelines<sup>3</sup>.

Radial velocities (RVs) have been measured by means of DAOSPEC (Stetson & Pancino 2008). Fig. 1 shows the radial velocities of the 89 stars observed in the direction of NGC 1806 as a function of the distance from the cluster center. The RV distribution of the entire sample ranges from  $+204.9$  to  $+336.8 \text{ km s}^{-1}$ . As can be seen in Fig. 1 a clump of 8 stars is clearly visible at  $RV=+228.6\pm 0.5 \text{ km s}^{-1}$  (gray squares). This value is fully compatible with  $RV=+225.0\pm 5.6 \text{ km s}^{-1}$  measured by

---

<sup>2</sup>However, it is worth recalling that Bastian et al. (2013) proposed an alternative mechanism to explain the chemical anomalies in GCs without resorting to multiple star formation episodes.

<sup>3</sup><http://www.eso.org/sci/software/pipelines/>

Olszewski et al. (1991) for star members of NGC 1806. The 8 stars are located within 2 arcmin from the cluster center, well within the tidal radius ( $r_c = 3.27'$ , Goudfrooij et al. 2011a) and within  $\sim 1.5\sigma$  from the mean cluster velocity. The above considerations suggest that the 8 selected stars are *bona fide* cluster members (this is also confirmed by the remarkable homogeneity in the derived iron abundance, see below).

Chemical abundances for a number of key elements (Fe, Ni, Mg, Al, Na, Si, Ca and Ti) have been obtained for the entire sample of giant stars by matching measured and theoretical equivalent widths (EWs) using the package GALA (Mucciarelli et al. 2013a)<sup>4</sup>, and we used spectral synthesis only for O, in order to model the forbidden O line at 6300.3 Å, affected by a close blending with a Ni transition. We refer the reader to Mucciarelli et al. (2013b) for a detailed description of the adopted line list, model atmospheres and determination of the uncertainties. EWs have been measured with the code DAOSPEC (Stetson & Pancino 2008), run through the automatic wrapper 4DAO (Mucciarelli 2013c)<sup>5</sup> that allows an analysis cascade of large sample of spectra and an easy, visual inspection of the Gaussian fit performed on each line of interest.

Effective temperatures ( $T_{eff}$ ) have been derived by means of the  $(J - K_s)_0 - T_{eff}$  relation of Gonzalez Hernandez & Bonifacio (2009) and adopting the color excess value of  $E(B-V) = 0.16$  mag quoted by Dirsch et al. (2000). Surface gravities have been derived with the Stefan-Boltzmann relation by assuming the photometric  $T_{eff}$ , the bolometric corrections of Alonso et al. (1999), a distance modulus of  $(m - M)_0 = 18.5$  mag (Alves 2004) and a mass of  $1.5M_\odot$ , according to a 1.75 Gyr-old isochrone (the average value of the ages of the two MSTOs quoted by Mackey et al. 2008)<sup>6</sup>, metallicity  $Z = 0.004$  and solar-scaled chemical mixture from the BaSTI data set (Pietrinferni et al. 2004). Finally, the microturbulent velocities have been derived spectroscopically, by erasing any trend between Fe I abundance and line strength. Corrections for departure from LTE for the Na lines have been obtained by interpolating on the grid of Gratton et al. (1999). Table 1 lists the abundance ratios measured for each member star of NGC 1806. Details about the analysis and the discussion of the measured abundances for the entire sample will be reported in a forthcoming paper (A. Mucciarelli et al. 2014, in preparation).

– *The photometric data set:* We used a combination of HST Advanced Camera for Survey - Wide Field Camera (ACS/WFC) and Wide Field Camera 3 - UVIS channel (WFC3/UVIS) data. The ACS/WFC images (Prop ID: 10595; PI: Goudfrooij) were obtained with the F435W and F814W filters, while the F336W band was used for the WFC3/UVIS (Prop ID: 12257, PI: Girardi) exposures. The photometric reduction were performed by following the approach described in Dalessandro et al. (2014). The final catalog consists of stars detected in all bands. The resulting

---

<sup>4</sup><http://www.cosmic-lab.eu/gala/gala.php>

<sup>5</sup><http://www.cosmic-lab.eu/4dao/4dao.php>

<sup>6</sup>Even if the cluster is suspected to have a spread in age, the assumption of the average age to derive the stellar mass is not a crucial issue, because the proposed age spread of 300 Myr corresponds to a mass difference of  $\sim 0.08 M_\odot$ , with a negligible impact on the gravities ( $\sim 0.02$ ).

field of view corresponds almost to the entire area covered by the WFC3 array ( $\sim 160'' \times 160''$ ). Instrumental magnitudes were reported to the VEGAMAG photometric system by using standard procedures and zero points reported by Sirianni et al. (2005) for the ACS data set and in the WFC3 web page for the WFC3 sample. Instrumental coordinates were roto-translated to the absolute  $(\alpha, \delta)$  coordinate system using the stars in common with the 2MASS catalog. Figure 2 shows the  $(m_{F814W}; m_{F336W} - m_{F814W})$  CMD of NGC 1806 for the stars lying within about  $30''$  from the cluster center.

### 3. Searching for chemical inhomogeneities in NGC 1806

For the 8 stars considered to be *bona fide* members of NGC 1806, we obtained the following results:

1. No evidence of star-to-star variations in terms of iron and light elements has been found. The average iron abundance turns out to be  $[\text{Fe}/\text{H}] = -0.60 \pm 0.01$  dex ( $\sigma_{obs} = 0.02$  dex). The same level of homogeneity has been obtained for the light elements (O, Na, Al, Mg), which exhibit intrinsic spreads in all old, massive GCs, both in our Galaxy (Carretta et al. 2009a) and in the LMC (Mucciarelli et al. 2009). We carefully checked for the presence of intrinsic scatter by using the Maximum Likelihood algorithm described in Mucciarelli et al. (2012a), which calculates the mean and the intrinsic spread ( $\sigma_{int}$ , with their corresponding uncertainties) of a given abundance ratio by taking into account the uncertainties of each individual star. For all the measured abundance ratios, the target stars formally have  $\sigma_{int} = 0.0$ , pointing out a strict homogeneity in the chemical content of NGC 1806. The lack of any significant light element spread can be appreciated in Fig. 3, where the individual stars of NGC 1806 (dark gray squares) are compared to the stars observed in old Galactic and LMC GCs (Carretta et al. (2009a) and Mucciarelli et al. (2009), respectively) in the  $[\text{O}/\text{Fe}]$ – $[\text{Na}/\text{Fe}]$  plane.
2. Fig. 4 shows the average abundance ratios measured for the 8 cluster members and the abundance ratios for the surrounding LMC field stars, both for three elements (O, Na, Mg) involved in the well known chemical anomalies and for  $[\langle \text{Si, Ca, Ti} \rangle / \text{Fe}]$  which usually shows no star-to-star variations. Oxygen and magnesium abundances nicely agree with those measured for other  $\alpha$ -elements (Si, Ca, Ti), at variance with what was found in old GCs where the stars with light element anomalies show  $[\text{O}/\text{Fe}]$  and  $[\text{Mg}/\text{Fe}]$  abundance ratios systematically lower than the other  $\alpha$ -elements. In addition, the abundance ratios measured in NGC 1806 well resemble those derived in the surrounding field stars (which show solar-scaled abundances, on average). Generally, in an old GC showing light-elements spread, stars with chemistry similar to that of the field are considered to be first generation stars, while those with significant light element differences are labeled as second generation stars. In the case of NGC 1806, the good agreement between cluster and field stars suggests that all the observed cluster members formed in the first episode of star formation.

3. At odds with what is typically found in old GCs properly observed in the U band (or similar filters, see e.g. the cases of M4 by Marino et al. (2008) and NGC 6362 by Dalessandro et al. 2014), the  $(m_{F814W}; m_{F336W} - m_{F814W})$  CMD of NGC 1806 does not exhibit any appreciable broadening or splitting of the RGB (see Fig. 2). In this plane possible RGB splittings are essentially driven by the intrinsic variations of C and N abundances, because the spectral region covered by the F336W filter (centered around  $\sim 3360 \text{ \AA}$ ) is dominated by strong CN and NH molecular bands (Sbordone et al. 2011). The distribution of the  $(m_{F336W} - m_{F814W})$  color residuals calculated with respect to the RGB mean ridge line (see the inset in Fig. 2) is fully compatible with the photometric uncertainties. This result suggests that no variations in the C and N abundances occur in the stellar population of NGC 1806.

Although the size of the presented spectroscopic sample is admittedly small, we note that chemical anomalies as large as those observed in the Galactic GCs have been detected in old LMC GCs (namely NGC 1786, NGC 2210 and NGC 2257, Mucciarelli et al. 2009) on the basis of samples of similar size. On the other hand, in old GCs the second generation stars numerically dominate the cluster population (accounting for  $\sim 50\%$ – $70\%$  of the entire stellar content; Carretta et al. 2009a). Thus, if two distinct stellar populations were present in NGC 1806, we would have expected to observe  $\sim 4$ – $6$  stars with significant light element abundance differences. Also, the remarkable chemical similarity between the cluster and the surrounding field stars rules out the possibility that all the observed stars are second generation stars.

#### 4. Discussion and conclusions

The presence of bimodal or extended MSTOs observed in some Magellanic intermediate-age clusters and the chemical anomalies in light element abundances observed in old stellar clusters have been suggested to have the same origin (Goudfrooij et al. 2009; Keller et al. 2011): they could be the fingerprint of self-enrichment processes operated by intermediate-mass AGBs and/or fast-rotating massive stars over a short timescale at the epoch of the cluster formation. Hence, stars in clusters with extended MSTOs should exhibit significant light element abundance variations. The analysis of the chemical and photometric properties of the bimodal MSTO cluster NGC 1806 presented in this Letter instead, indicates a high level of chemical homogeneity in the cluster population, drawing a simple conclusion: *NGC 1806 does not show major evidence of multiple stellar populations as observed in old GCs* (included the old LMC GCs that exhibit chemical anomalies like those of the Galactic ones, Mucciarelli et al. 2009). Also, we recall that NGC 1806 has a present-day mass ( $M=1.07 \cdot 10^5 M_{\odot}$ , Goudfrooij et al. 2011b) comparable with those of the Galactic/LMC old clusters where the chemical anomalies have been observed.

Hence, there is no evidence that NGC 1806 underwent any self-enrichment process. This suggests univocally that bimodal MSTO and light element chemical anomalies cannot be explained within the same framework. Moreover, a significant broadening of the MSTO has been observed

only in a relatively small range of cluster ages, between 1 and 2 Gyr (see Figure 1 in Keller et al. 2011), while it is not visible in younger clusters at odds with what would be expected if it was a common feature of the cluster formation process. Indeed, for example, the young, massive LMC cluster NGC 1866 has been found to harbor a mono-age (Bastian & Silva-Villa 2013) and mono-metallic (Mucciarelli et al. 2011) stellar population.

In light of this finding, other solutions (invoking or not an intrinsic age spread but always preserving the homogeneity in the chemical abundances) should be envisaged to explain this class of globulars (see e.g. the extended discussions provided by Santiago et al. 2002; Bekki & Mackey 2009, and Keller et al. 2011). As suggested by Bekki & Mackey (2009), new episodes of star formation could be triggered by the merging or the interaction between an already existing cluster (corresponding to the faintest MSTO) and a giant molecular cloud. While no explicit predictions are provided for the chemical content of a GC formed through this mechanism, the authors do not exclude that the pollution by AGB stars could occur and that the stars formed from the second burst of star formation could display the same kind of chemical anomalies in light elements observed in old GCs. However, this could be in disagreement with our findings in NGC 1806.

Another possibility is that bimodal MSTO GCs are the result of a merging event between the components of a binary/multiple cluster system, formed by the collapse of the same molecular cloud but with an initial difference in their ages. This would naturally account for chemical homogeneity in clusters with different ages. The LMC and SMC harbor a significant population of candidate binary/multiple clusters (see Mucciarelli et al. 2012b, and references therein). This scenario could explain only the bimodal MSTOs, but cannot account for clusters with an extended MSTO without discrete sub-structures.

Other mechanisms, not requiring an age spread, could be the solution and they should be better investigated. Bastian & de Mink (2009) first proposed that the effect of rotation in the evolution of MS stars with  $M > 1.2 M_{\odot}$  can account for the observed MSTO: for a coeval population, fast rotating MS stars evolve to lower  $T_{eff}$ , with respect to non-rotating stars, thus mimicking a redder MSTO. However, by including the effect of the rotation in the calculation of the stellar lifetimes (an effect neglected by Bastian & de Mink 2009) Girardi et al. (2011) conclude that rotating stars are slightly bluer and brighter than non-rotating ones, but this effect is not sufficient to mimic extended MSTOs like those observed in the Magellanic GCs. On the other hand, the recent investigation by Yang et al. (2013) leads to the opposite result. Their calculations show that rotating stars are colder and evolve faster than non-rotating stars. In particular, Yang et al. (2013) emphasize that the efficiency of rotational induced mixing (a mechanism that is still debated) is a crucial parameter to reproduce the observed MSTO. Thus, they conclude that rotation can, in principle, lead to a dual or broad MSTO. Further investigations of this process and any alternative scenarios are needed and urged to finally understand the origin of the observed MSTO morphologies.

We thank the anonymous referee for useful comments. This research is part of the project COSMIC-LAB (Web site: <http://www.cosmic-lab.eu>) funded by the European Research Council

(under contract ERC-2010-AdG-267675).

## REFERENCES

- Alonso, A., Arribas, S., & Martinez-Roger, C., 1999, *A&As*, 140, 261
- Alves, D. R., 2004, *New Astro. Rev.*, 48, 659
- Bastian, N., & de Mink, S. E., 2009, *MNRAS*, 398, L11
- Bastian, N., Lamers, H. J. G. L. M., de Mink, S. E., Longmore, S. N., Goodwin, S. P., & Gieles, M., 2013, *MNRAS*, 436, 2398
- Bastian, N., & Silva-Villa, E., 2013, *MNRAS*, 431, 122
- Bekki, K., & Mackey, A. D., 2009, *MNRAS*, 394, 124
- Carretta, E., et al., 2009, *A&A*, 505, 117
- Carretta, E., Bragaglia, A., Gratton, R., D’Orazi, V., & Lucatello, S., 2009, *A&A*, 505, 139
- Dallessandro, E., Massari, D., Bellazzini, M., Miocchi P., Mucciarelli, A., Salaris, M., Cassisi, S., Ferraro, F. R., & Lanzoni, B., 2014, *ApJ*, 791L, 4
- Decressin, T., Baumgardt, H., Charbonnel, C., & Kroupa, P., 2010, *A&A*, 516, 73
- D’Ercole, A., Vesperini, E., D’Antona, F., McMillan, S. L. W., & Recchi, S., 2008, *MNRAS*, 391, 825
- Dirsch, B., Richtler, T., Gieren, W. P., & Hilker, M., 2000, *A&A*, 360, 133
- Glatt, K., et al., 2008, *AJ*, 136, 1703
- Girardi, L., Eggenberger, P., & Miglio, A., 2011, *MNRAS*, 412, L103
- Gonzalez Hernandez, J. I., & Bonifacio, P., 2009, *A&A*, 497, 497
- Goudfrooij, P., Puzia, T. H., Kozhurina-Platais, V., & Chandar, R., 2009, *AJ*, 137, 4988
- Goudfrooij, P., Puzia, T. H., Kozhurina-Platais, V., & Chandar, R., 2011, *ApJ*, 737, 3
- Goudfrooij, P., Puzia, T. H., Chandar, R., & Kozhurina-Platais, V., 2011, *ApJ*, 737, 4
- Gratton, R. G., Carretta, E., Eriksson, K. & Gustafsson, B., 1999, *A&A*, 350, 955
- Gratton, R. G., Carretta, E., & Bragaglia, A., 2012, *A&ARv*, 20, 50
- Keller, S. C., Mackey, A. D., & Da Costa, G. S., 2011, *ApJ*, 731, 22



- Mackey, A. D., & Broby Nielsen, P., 2007, MNRAS, 379, 151
- Mackey, A. D., Broby Nielsen, P., Ferguson, A. M. N., & Richardson, J. C., 2008, ApJ, 681L, 17
- Marino, A. F., Villanova, S., Piotto, G., Milone, A. P., Momany, Y., Bedin, L. R., & Medling, A. M., 2008, A&A, 490, 625
- Milone, A. P., Bedin, L. R., Piotto, G., & Anderson, J., 2009, A&A, 497, 755
- Mucciarelli, A., Origlia, L., Ferraro, F. R., Maraston, C., & Testa, V., 2006, ApJ, 646, 939
- Mucciarelli, A., Ferraro, F. R., Origlia, L., & Fusi Pecci, F., 2007, AJ, 133, 2053
- Mucciarelli, A., Origlia, L., Ferraro, F. R., & Pancino, E., 2009, ApJ, 695L, 134
- Mucciarelli, A., Cristallo, S., Brocato, E., Pasquini, L., Straniero, O., Caffau, E., Raimondo, G., Kaufer, A., Musella, I., Ripepi, V., Romaniello, M., & Walker, A. R., 2011, MNRAS, 413, 837
- Mucciarelli, A., Bellazzini, M., Ibata, R., Merle, T., Chapman, S. C., Dalessandro, E., & Sollima, A., 2012, MNRAS, 426, 2889
- Mucciarelli, A., Origlia, L., Ferraro, F. R., Bellazzini, M., & Lanzoni, B., 2012, ApJ, 746L, 19
- Mucciarelli, A., Pancino, E., Lovisi, L., Ferraro, F. R., & Lapenna, E., 2013, ApJ, 766, 78
- Mucciarelli, A., Bellazzini, M., Catelan, M., Dalessandro, E., Amigo, P., Correnti, M., Cortés, C. & D’Orazi, V., 2013, MNRAS, 435, 3667
- Mucciarelli, A., 2013, arXiv1311.1403
- Olszewski, E. W., Schommer, R. A., Suntzeff, N. B., & Harris, H. C., 1991, AJ, 101, 515
- Pasquini, L., et al., 2000, SPIE, 4008, 129
- Pietrinferni, A., Cassisi, S., Salaris, M., & Castelli, F., 2004, ApJ, 612, 168
- Rubele, S., Girardi, L., Kozhurina-Platais, V., Kerber, L., Goudfrooij, P., Bressan, A., & Marigo, P., 2013, MNRAS, 430, 2774
- Santiago, B., Kerber, L., Castro, R., & de Grijs, R., 2002, MNRAS, 336, 139
- Sbordone, L., Salaris, M., Weiss, A., & Cassisi, S., 2011, A&A, 534, 9
- Skrutskie, M. F., et al., 2006, AJ, 131, 1163
- Sirianni, M., et al., 2005, PASP, 117, 1049
- Stetson, P. & Pancino, E., 2008, PASP, 120, 1332

Valcarce, A. A. R., & Catelan, M., 2011, *A&A*, 533, 120

Ventura, P., D’Antona, F., Mazzitelli, I., & Gratton, R., 2001, *ApJ*, 550, 65

Yang, W., Meng, X., Bi, S., Tian, Z., Li, T., & Liu, K., 2011, *ApJ*, 731L, 37

Yang, W., Bi, S., Meng, X., & Liu, K., 2013, *ApJ*, 776, 112

Table 1.

Star	RA (J2000)	Dec (J2000)	J	K	RV (km s <sup>-1</sup> )	$T_{eff}$ (K)	log g	$v_{turb}$ (km s <sup>-1</sup> )	[Fe/H] (dex)
NGC 1806-25	75.5685190	-67.9808206	13.68	12.65	230.6±0.	3920	0.7	1.60	-0.62±0.04
NGC 1806-27	75.5639398	-67.9835530	13.70	12.69	229.1±0.	3990	0.7	1.60	-0.58±0.04
NGC 1806-29	75.5152945	-67.9793630	13.74	12.74	229.4±0.	4000	0.7	1.70	-0.62±0.04
NGC 1806-30	75.5473719	-67.9918053	13.74	12.79	227.0±0.	4120	0.8	1.60	-0.58±0.05
NGC 1806-32	75.5162281	-67.9868209	13.76	12.80	226.1±0.	4090	0.8	1.50	-0.59±0.05
NGC 1806-40	75.5323035	-67.9868328	14.28	13.35	229.0±0.	4150	1.0	1.60	-0.58±0.04
NGC 1806-33	75.5638527	-67.9949059	13.85	12.86	227.9±0.	4040	0.8	1.60	-0.61±0.11
NGC 1806-39	75.5908674	-67.9588433	14.13	13.22	229.3±0.	4220	1.0	1.60	-0.60±0.10
Star	[O/Fe] (dex)	[Na/Fe] (dex)	[Mg/Fe] (dex)	[Al/Fe] (dex)	[Si/Fe] (dex)	[Ca/Fe] (dex)	[Ti/Fe] (dex)	[Ni/Fe] (dex)	11
NGC 1806-25	+0.10±0.08	+0.11±0.14	0.06±0.07	+0.09±0.12	+0.15±0.10	+0.02±0.15	+0.09±0.18	-0.08±0.03	
NGC 1806-27	+0.04±0.07	+0.09±0.12	0.02±0.06	+0.14±0.09	+0.08±0.11	+0.09±0.12	+0.13±0.16	-0.13±0.04	
NGC 1806-29	+0.16±0.08	+0.09±0.12	-0.01±0.07	+0.11±0.09	+0.11±0.11	+0.14±0.13	+0.17±0.16	-0.15±0.04	
NGC 1806-30	+0.12±0.09	+0.10±0.13	0.06±0.08	+0.19±0.08	+0.03±0.11	+0.16±0.11	+0.25±0.15	-0.17±0.05	
NGC 1806-32	+0.10±0.07	+0.07±0.11	0.11±0.07	+0.19±0.09	+0.02±0.10	+0.13±0.11	+0.20±0.15	-0.16±0.04	
NGC 1806-40	+0.11±0.09	+0.03±0.09	0.06±0.08	+0.13±0.08	+0.07±0.11	+0.14±0.10	+0.12±0.15	-0.14±0.04	
NGC 1806-33	+0.12±0.12	+0.03±0.11	0.12±0.13	—	+0.16±0.13	+0.16±0.12	+0.15±0.17	-0.12±0.08	
NGC 1806-39	+0.14±0.12	+0.07±0.09	0.09±0.10	—	+0.14±0.12	+0.17±0.11	+0.14±0.14	-0.08±0.08	

Note. — Coordinates and magnitudes are from Mucciarelli et al. (2006). The abundance uncertainties include the internal error and that due to the atmospheric parameters.

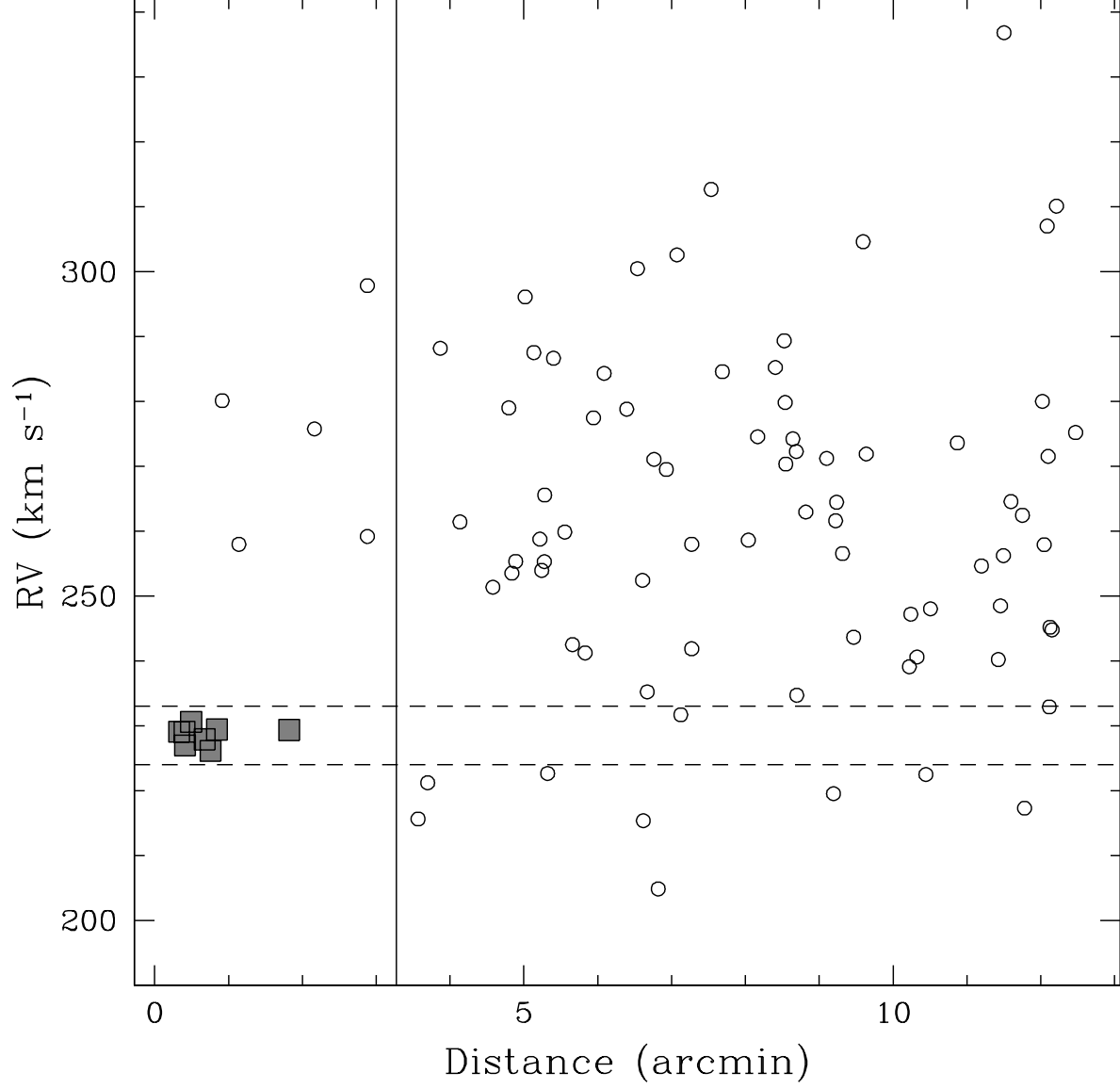


Fig. 1.— Radial velocities as a function of the distance from the cluster center for the entire spectroscopic sample (gray squares are the cluster member stars and open circles the LMC field stars). The dashed horizontal lines indicate the  $\pm 3\sigma$  level from the average RV of the cluster. The vertical line indicates the tidal radius of NGC 1806 ( $r_t = 3.27'$ , Goudfrooij et al. 2011a).

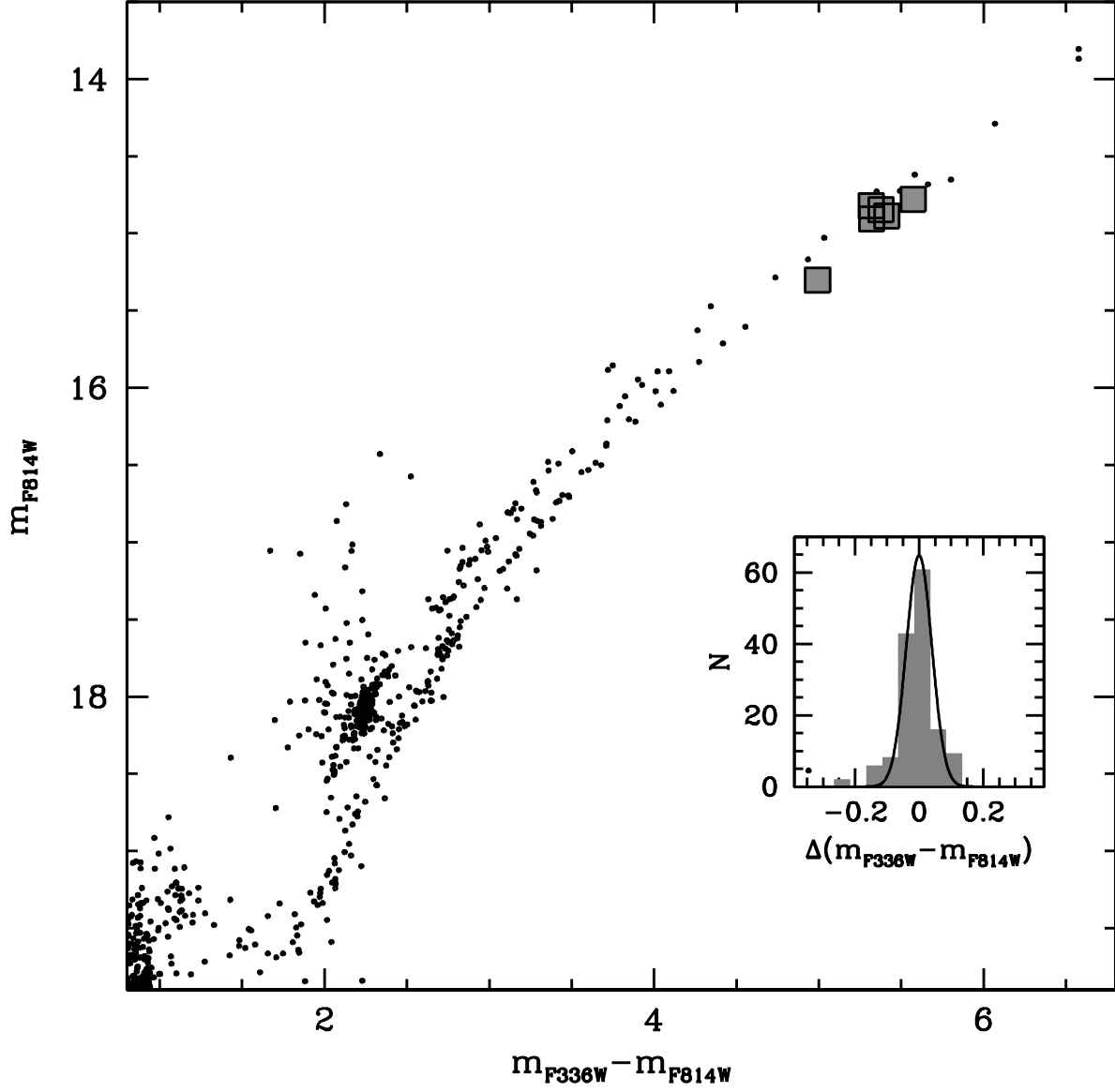


Fig. 2.—  $(m_{F814W}; m_{F336W} - m_{F814W})$  color-magnitude diagram obtained with HST data for the innermost 30 " from the cluster center. Gray squares are the spectroscopic targets lying in HST field of view. The inset shows the histogram of the  $(m_{F336W} - m_{F814W})$  color residuals calculated with respect to the RGB mean ridge line, with over-imposed the distribution of the photometric uncertainties.

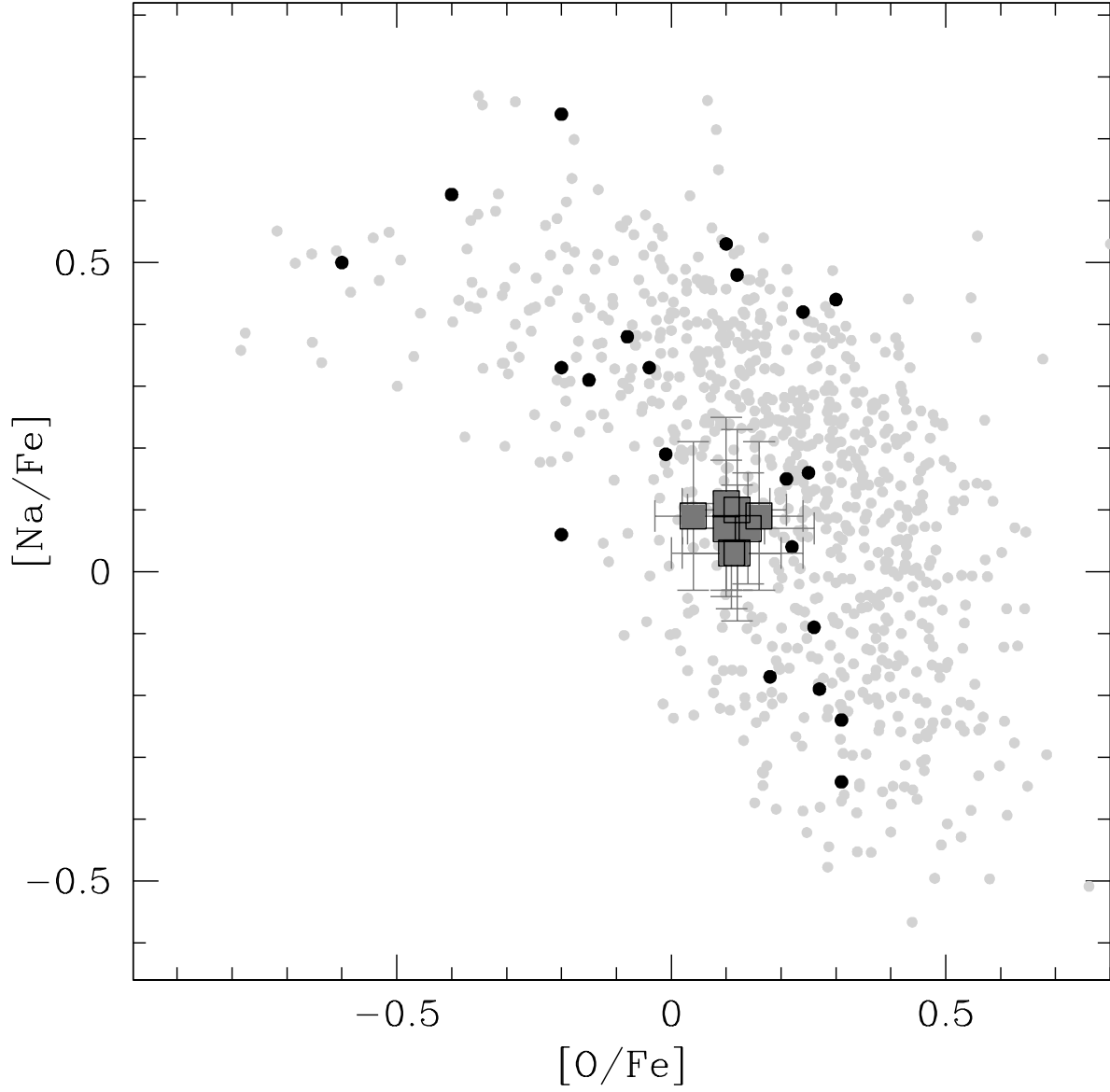


Fig. 3.—  $[\text{Na}/\text{Fe}]$  as a function of  $[\text{O}/\text{Fe}]$  for the 8 members of NGC 1806 (dark gray squares), compared to the stars in old Milky Way (light gray points, Carretta et al. 2009a) and LMC (black points, Mucciarelli et al. 2009) GCs.

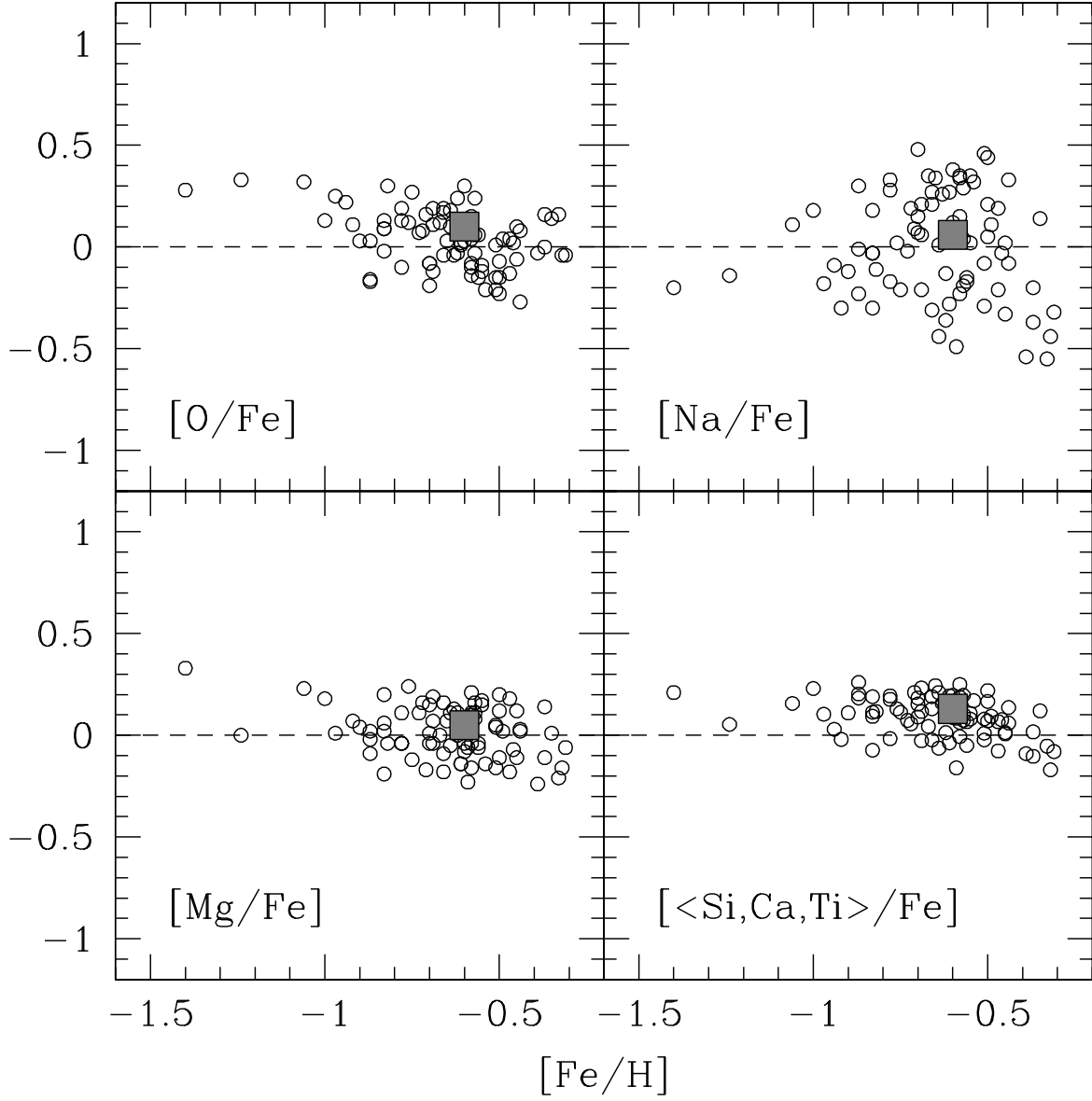


Fig. 4.— Comparison between the average values of the  $[\text{O}/\text{Fe}]$ ,  $[\text{Na}/\text{Fe}]$ ,  $[\text{Mg}/\text{Fe}]$  and  $[<\text{Si,Ca,Ti}>/\text{Fe}]$  abundance ratios for NGC 1806 (gray squares) and for the surrounding field stars (open circles).